Available online at www.sciencedirect.com
ScienceDirect
Bioorganic & Medicinal Chemistry 16 (2008) 5473–5481
Bioorganic & Medicinal Chemistry

Design, synthesis, and QSAR studies of novel lysine derives as amino-peptidase N/CD13 inhibitors

Qiang Wang,[a] Maoying Chen,[a] Huawei Zhu,[a] Jie Zhang,[a] Hao Fang,[a] Binghe Wang[b] and Wenfang Xu[a,*]

[a]*Department of Medicinal Chemistry, School of Pharmacy, Shandong University, Ji'nan, Shandong 250012, PR China*
[b]*Department of Chemistry, Georgia State University, Atlanta, GA 30303, USA*

Received 30 January 2008; revised 6 April 2008; accepted 8 April 2008
Available online 11 April 2008

Abstract—A series of novel L-lysine derivatives were designed, synthesized, and assayed for their inhibitory activities on amino-peptidase N (APN)/CD13 and matrix metalloproteinase-2 (MMP-2). The preliminary biological test showed that most of the compounds displayed a high inhibitory activity against MMP-2 and a low activity against APN except compound **B6** which exhibited good potency (IC_{50} = 13.2 μM) similar with APN inhibitor Bestatin (IC_{50}=15.5 μM), and could be used as lead compound in the future.

1. Introduction

As a zinc-dependent endopeptidase, amino-peptidase N (APN) is also known as CD13. Scientific research has been found that APN is over-expressed on tumor cells and play an important role in extracellular matrix degradation and invasion of tumor cells. Therefore, APN has been a target for anticancer agents design. Since 1976, a great amount of natural inhibitors have been found to bind APN with high affinity (Fig. 1), including Bestatin (**1**),[1] probestin (**2**),[2] amastatin (**3**),[3] actinonin (**4**),[4] phebestin (**5**),[5] lapstatin (**6**),[6] AHPA-Val (**7**),[7] leuhistin (**8**),[8] curcumin (**9**)[9], and pasmmaplin A (**10**).[10]

Our group has synthesized a series of 3-galloylamido-*N*′-substituted 2,6-piperidinedione-*N*-acetamide peptidomimetics and found that the two target compounds displayed a similar inhibitory activity compared with Bestatin.[11] In our on-going work, the strategy of computer-aided molecular design has been used for developing new peptidomimetics as APN inhibitors and the docking studies have been done with natural APN inhibitors listed in Figure 1. The results suggested that the APN inhibitors can be divided into three parts. *Part A*: hydrophobic fragment; *Part B*: zinc binding group (ZBG); and *Part C*: heterocyclic rings or hydrophobic groups (Fig. 2).

According to the literature, ZBG (part 2) could be carboxylic acid and hydroxymate. Then, the next step we need to do should be not only the determination of the hydrophobic fragment or heterocycle as part A and part C, but also the choosing of a linker to connect the three parts. In our preliminary studies, L-lysine was selected as a linker due to its structure containing two amino groups and one carboxylic acid which can be used as ZBG. Therefore, a series of L-lysine derivatives could be designed with different α-amino substitution and N^6-amino substitution. In this study, we reported the preparation and in vitro APN inhibition studies of N^6-Cbz substituted L-lysine derivatives.

2. Chemistry

The synthesis of target compounds is shown in Scheme 1. The N^6-amino of L-lysine was selectively protected by Cbz (carbobenzoxy) and then esterificated with HCl in methanol to generate methyl 2-amino-6-(benzyloxycarbonylamino)hexanoate hydrochloride. Then, 10 different aromatic acids were converted to acyl chloride and reacted with 2-amino group of L-lysine. Finally, the ester functional group was hydrolyzed with NaOH/H_2O in methanol or treated with NH_2OK in methanol to get hydroxymic acid.

Keywords: Lysine derivatives; Synthesis; APN/CD13; Inhibitor; QSAR.
* Corresponding author. Tel./fax: +86 531 88382264; e-mail: xuwenf@sdu.edu.cn

0968-0896/$ - see front matter © 2008 Elsevier Ltd. All rights reserved.
doi:10.1016/j.bmc.2008.04.012

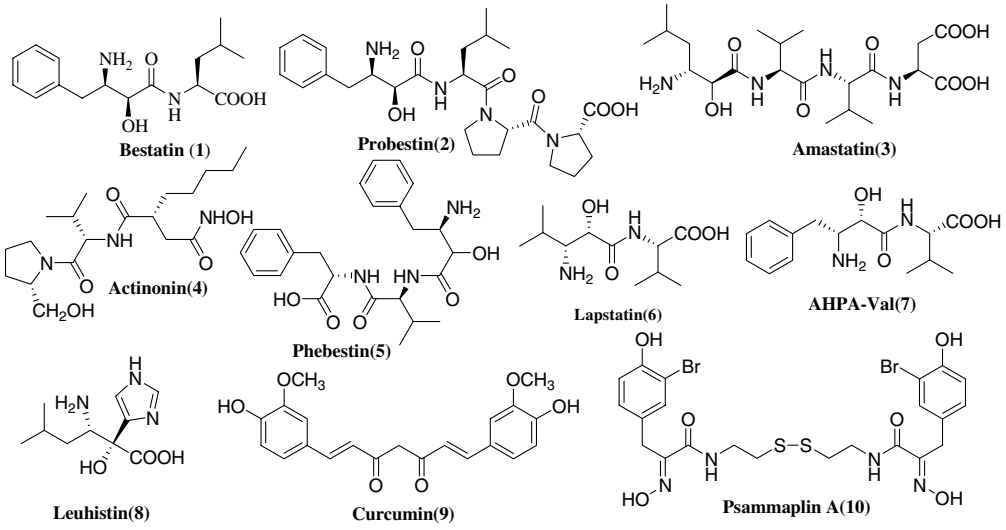

Figure 1. Natural inhibitors of APN.

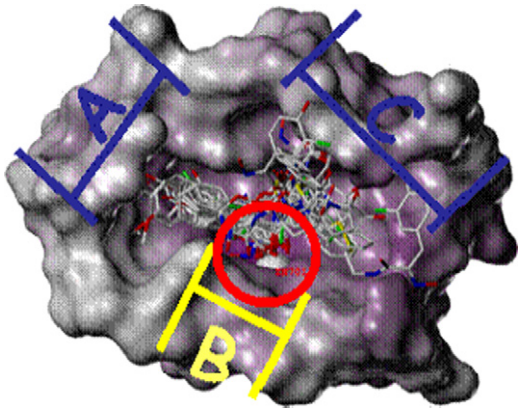

Figure 2. Docking the inhibitors showed in Figure 1 to APN.

3. Results and discussion

All the target compounds were tested for their inhibitory ability against APN. Considering that matrix metalloproteinases-2 (MMP-2) also belong to the zinc-dependent metalloproteinase and are associated with a malignant tumor, the inhibitory studies were performed on both APN and MMP-2 so as to identify the selectivity of the target compounds.

From the results listed in Table 1, it can be found that compound **B6** (IC_{50} = 13.2 μM) is the most potent APN inhibitor in all the target compounds, which showed an inhibition similar to that of Bestatin (IC_{50} = 15.5 μM). The inhibitory activity of the B series (R_2:-NHOH) were generally better than the A series (R_2:-OH). It may be caused by the hydroxymate residue in B the series, which is a more strong zinc binding group than the carboxylic acid. For the substitution of α-amino in L-lysine (R_1), a six-membered aromatic ring seems to be better than a five-membered aromatic ring.

However, most of the target compounds exhibited a better inhibitory activity on MMP-2 than APN except **B6**. This phenomenon was also found in our previous studies on 3-galloylamido-*N*′-substituted 2,6-piperidinedione-*N*-acetamide peptidomimetics.[11] The possible reason may be the difference of the three-dimensional structure of active sites of APN and MMP-2. By taking

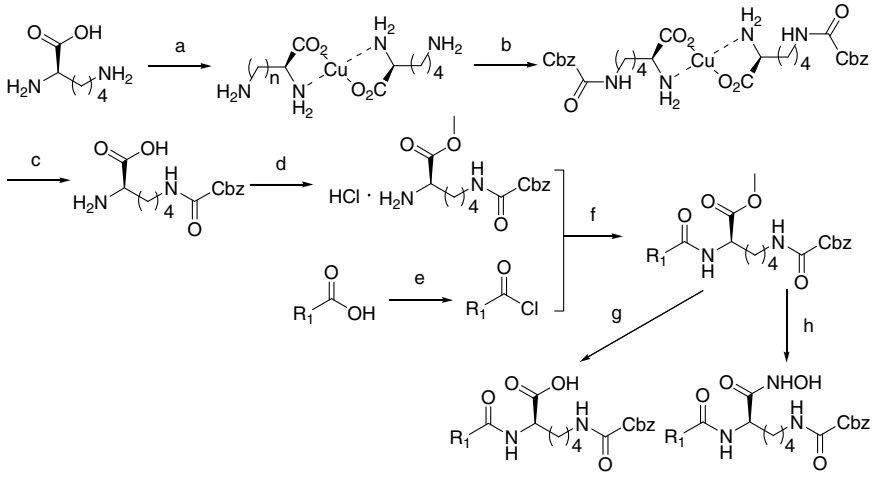

Scheme 1. Reagents and conditions: (a) $CuCO_3Cu(OH)_2$, 1.2 N HCl, H_2O, 80–90 °C; (b) $NaHCO_3$, CbzCl, 25 °C; (c) EDTA SS, 25 °C; (d) MeOH, HCl, 25 °C; (e) oxalyl chloride, CH_2Cl_2, ice-salt bath; (f) Et_3N, CH_2Cl_2, 0 °C; (g) 2 N NaOH, 1 N HCl, 25 °C; (h) NH_2OK, MeOH, 25 °C.

Table 1. The structure and inhibitory activities of compounds against APN and MMP-2

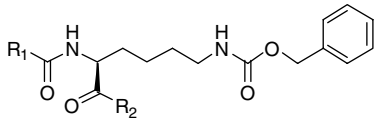

Compound	R_1	R_2	IC_{50} (μM)		QSAR of model C		
			MMP-2	APN	pIC_{50}		Res.
					Act.	Pre.	
A1	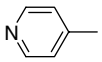	–OH	8.76	291.6	3.54	3.58	−0.04
A2		–OH	2.93	197.4	3.70	3.71	−0.01
A3		–OH	8.49	1120.7	2.95	2.96	−0.01
A4		–OH	3.14	166.8	3.78	3.74	0.03
A5		–OH	12.7	1247.2	2.90	2.89	0.01
A6	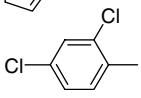	–OH	17.8	127.2	3.90	3.90	0.00
A7	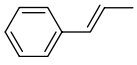	–OH	50.5	215.1	3.67	3.67	0.00
A8	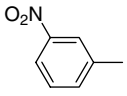	–OH	7.48	110.8	3.96	3.95	0.01
A9	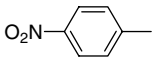	–OH	19.2	202.2	3.69	3.69	0.00
A10	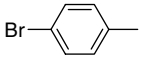	–OH	13.1	188.0	3.73	3.73	0.00
B1	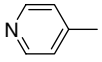	–NHOH	25.5	91.2	4.04	3.99	0.05
B2		–NHOH	14.3	97.0	4.01	4.02	−0.01
B3		–NHOH	8.08	158.7	3.80	3.77	0.03
B4		–NHOH	8.0	94.3	4.03	4.05	−0.02
B5		–NHOH	12.6	159.1	3.80	3.83	−0.03
B6	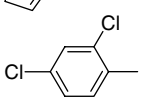	–NHOH	170.0	13.2	4.88	4.88	0.00
B7	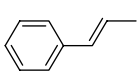	–NHOH	3.54	569.6	3.24		
B8	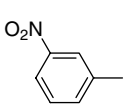	–NHOH	11.7	95.8	4.02	4.03	−0.01

(*continued on next page*)

Table 1 (*continued*)

Compound	R_1	R_2	IC_{50} (μM)		QSAR of model C		
			MMP-2	APN	pIC_{50}		Res.
					Act.	Pre.	
B9	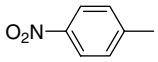	–NHOH	32.0	107.9	3.97	3.99	−0.02
B10	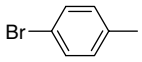	–NHOH	9.94	111.9	3.95	3.94	0.01
	Bestatin		21.96	15.5			

an insight into the active site of APN(PDB code: 1HS6) and MMP-2 (PDB code: 1HOV, 1CK7, 1QIB), we found that the active site of APN was more deeper than the active site of MMP-2, which leads to the difficulty to access the active site of APN in most compounds.

4. SAR studies

4.1. Dataset and molecular modeling

We chose **B6** as a template molecule and tried to find the pharmacophoric conformation. First, all the conformations of B6 searched by SYSTEM SEARCH in Sybyl7.0 were docked to the active site of APN. From the results, we found that there were two possibilities: (1) *Conformation I:* R_1 stretched into pocket A and Cbz stretched into pocket C; (2) *Conformation II:* Cbz stretched into pocket A and R_1 stretched into pocket C. The best docked conformation was picked out for each of them (Fig. 3). Second, we take an energy analysis for the two conformations (Table 2). In addition, considering the conformation of Bestatin binding to APN in the X-ray crystal, the benzene ring of Bestatin stretched into pocket A was more close to its ZBG; we chose *conformation I* as the pharmacophoric conformation of **B6**, which has a lower energy and its R_1 is more near to R_2 (Fig. 4). Third, the template molecule **B6** was taken and the rest of the molecules were aligned to it by the DATABASE ALIGNMENT method in Sybyl (Fig. 5).

The QSAR studies were carried out with CoMFA[12] of Sybyl. The IC_{50} values were converted into pIC_{50} according to the formula: $pIC_{50} = -\lg IC_{50}$.

Considering that compounds **A7** and **B7** are different from others, four models of QSAR have been studied so as to obtain reasonable statistics. This is because there is an olefin bond between the aromatic ring and the amide in the R_1 position of A7 and B7, which leads to the significant structural difference in comparison to other compounds. Therefore, results of the CoMFA model will also be different irrespective to the training set including them.

The steric and electrostatic CoMFA fields were calculated at each lattice intersection of a regularly spaced grid of 2.0 Å in all the three dimensions within a defined region. A sp^3 carbon atom with +1.00 charge was used as a probe atom. The steric and electrostatic fields were truncated at +30.00 kcal mol^{-1}, and the electrostatic fields were ignored at the lattice points with maximal steric interactions.

PLS method was used to linearly correlate the CoMFA fields to the inhibitory activity values. The cross-validation analysis was performed using the leave one out (LOO) method in which one compound is removed from the dataset and its activity is predicted using the model derived from the rest of the dataset. The cross-validated r^2 that resulted in optimum number of components and lowest standard error of prediction were considered for further analysis.

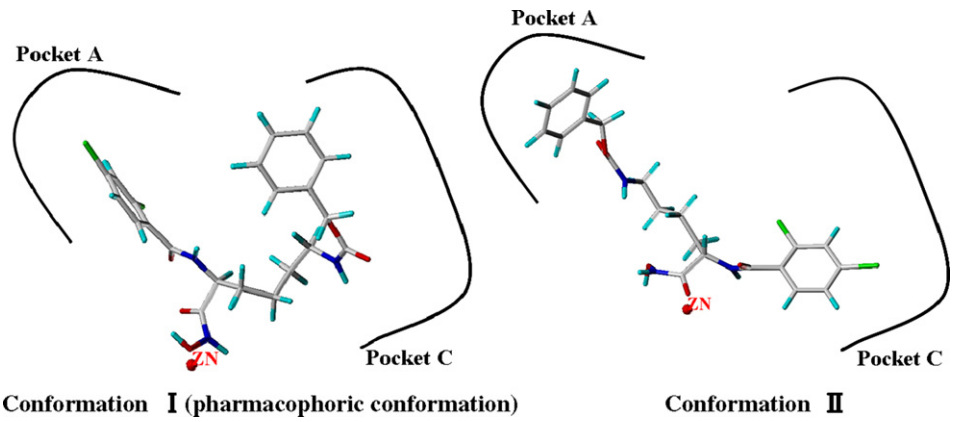

Figure 3. The docking results of **B6**.

Table 2. The energy analysis of conformation I and conformation II

Energy analysis (kcal mol^{-1})	Conformation I	Conformation II
Bond stretching energy	0.803	0.848
Angle bend energy	3.952	4.283
Torsional energy	37.009	40.673
Out of plane bending energy	0.115	0.180
1–4 Van der Waals energy	6.319	5.524
Van der Waals energy	14.831	24.827
Total energy	63.029	76.334

4.2. Results and discussion

The LOO cross-validated q^2 of the CoMFA model C is 0.737. The non cross-validated r^2 for the model established by the study is 0.997. The value of the variance ratio $F(n_1 = 10,\ n_2 = 8)$ is 289.708 and the standard error of the estimate (SEE) is 0.033. The contribution of electrostatic and steric is 50.4% and 49.6%, respectively Finally, model C had a good predictability as shown in, Figure 7.

According to the results in Table 3, the CoMFA model C is the best one and the coefficient contour plots of CoMFA model C are shown in Figure 7. It suggested that the influence of steric field on APN inhibitory activity is mainly located in the R_1 and R_2 positions (Fig. 6(a)). The green region surrounded the R_2 group which indicated that the bulky group of the B series (R_2:-NHOH) is better than that of the A series (R_2:-OH), while the yellow area was mainly around R_1, which accorded with the nature of part A in docking studies. This is because part A is a small pocket and the bulky group substitution would be unfavorable for APN inhibition. For example, compounds A7 and B7 showed a low APN inhibitory activity, which contain the larger substitution of styrene in R_1 position. In Figure 6(b), the blue area was mainly surrounded by the aromatic ring of R_1 position and suggested that electronegativity groups, such as Cl, Br, and NO_2, may enhance its activity. Based on our result, 2,4-dichloro substitution exhibited better inhibitory activities on APN, and compound **B6** is the most potent and selective compound in these L-lysine derivatives.

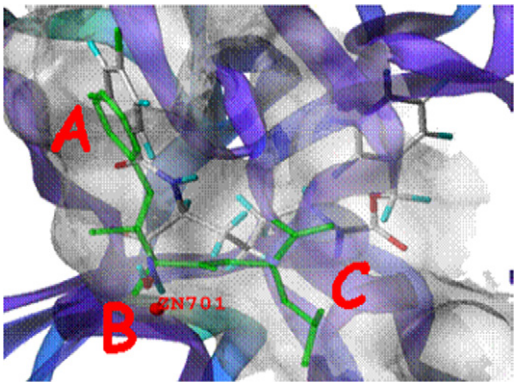

Figure 4. Pharmacophoric conformation of **B6** (Bestatin in the X-ray crystal is showed in green).

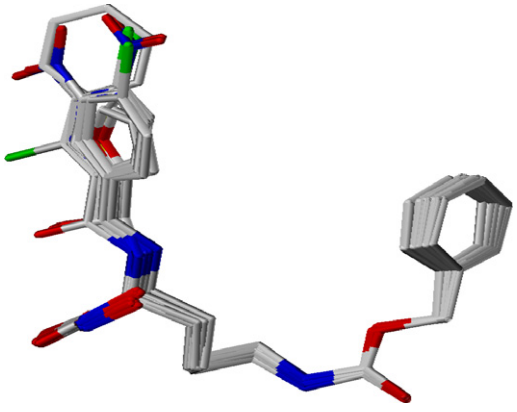

Figure 5. Superposition of 20 inhibitors for CoMFA construction.

5. Conclusions

In summary, we developed a series of novel L-lysine derivatives as potential APN inhibitors. Among them, compound **B6** not only exhibited a similar inhibitory activity compared with natural APN inhibitor Bestatin, but also showed a significant selectivity for APN over MMP-2. Therefore, **B6** could be a lead compound for us to search new L-lysine derivatives as APN inhibitors.

6. Experimental

6.1. APN inhibition assay

IC_{50} values against APN were determined as previously described and by using L-Leu-*p*-nitroanilide as a substrate and Microsomal amino-peptidase from Porcine Kidney Microsomes (Sigma) as the enzyme in 50 mM PBS, pH 7.2, at 37 °C. The hydrolysis of the substrate was monitored by following the change in the absorbance measured at 405 nm with the UV–vis spectrophotometer Pharmacia LKB, Biochrom 4060. All the solutions of the inhibitors were prepared in the assay buffer, and the pH was adjusted to 7.5 by the addition of 0.1 M HCl or 0.1 M NaOH. All the inhibitors were preincubated with APN for 30 min at room temperature. The assay mixture, which contained the inhibitor solution (concentration dependent on the inhibitor), the enzyme solution (4 μg/mL final concentration), and the assay buffer, was adjusted to 200 μL.

6.2. MMP inhibition assay

Gelatinase A (MMP-2) and TNBS were purchased from Sigma, and the substance was synthesized as described by Vijaykumar et al. The gelatinase, substance, and inhibitor were dissolved in sodium borate (pH 8.5, 50 mmol/L) and incubated for 30 min at 37 °C, and then 0.03%TNBS was added and incubated for another 20 min, the resulting solution was detected under 450 nm wavelength to gain absorption.

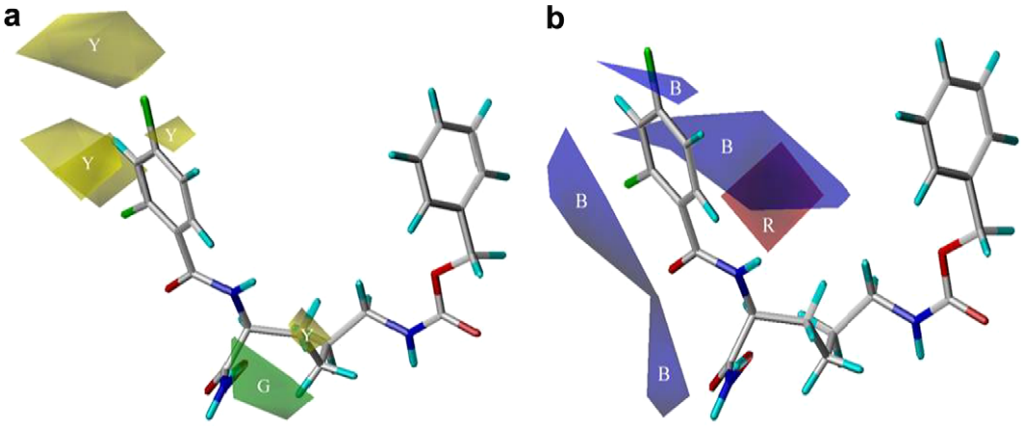

Figure 6. CoMFA coefficient contour map of model C (B6 is in the background). (a) Green (G) is the more bulky region, yellow (Y) is the less bulky region; (b) red (R) color represents the negative charge region, blue (B) is the positive charge region.

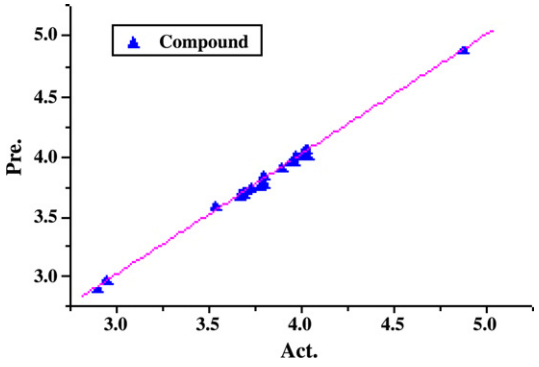

Figure 7. The predictability of the CoMFA model C.

6.3. Chemistry: general procedures

6.3.1. N^6-[(Benzyloxy)carbonyl]-L-lysine (1). The title compound was prepared as described by Shen Zongxuan.[13]

The starting materials, cupric subcarbonate (4.3 g, 18.1 mmol) and 1.2 N HCl (24 ml) were dissolved in water (36 ml). To this mixture, L-lysine (4.3 g, 29.4 mmol) was added and heated to 80–90 °C. The resulting pale blue mixture was gently refluxed for 1 h. The warm reaction mixture was filtered using vacuum and washed with hot water (3× 10 ml). The combined aqueous filtrates were cooled to room temperature. $NaHCO_3$ (3.37 g, 40.1 mmol) was added to the mixture followed by a solution of benzylchloroformate (5.4 g, 31.8 mmol) in methylbenzol (30 ml) dropwise over 3 min period. The reaction mixture was stirred for 24 h, filtered, and washed with water (3× 30 ml). The solid filter cake was dried in a vacuum dryer. The blue solid cake was dissolved in EDTA SS (100 ml) and stirred for 12 h, filtered and washed with water, repeated this step again to get a white microcrystalline powder (yield 88%, mp 230–236 °C).

6.3.2. 2-Amino-6-(benzyloxycarbonylamino)hexanoate hydrochloride (2). This compound was prepared as described by Jordis[14] with compound **1**.

6.3.3. N^6-[(benzyloxy)carbonyl]-N^2-isonicotinoyl-L-lysine hexanoate (3). To a (100 ml) two-necked flask equipped with a stirring oar was dropwise added 2.0 g of isonicotinic acid dissolved with 40 ml methylene chloride followed by a solution of oxalyl chloride(1.1 equiv) in methylene chloride (10 ml) over a 10-min period. The temperature was kept below −5 °C by ice-salt bath. The reaction mixture was stirred for 5 h and then condensed by rotary evaporation to remove methylene chloride and excess oxalyl chloride.

Compound **2** (3.0g) and TEA (2.0 equiv) were dissolved in methylene chloride (50 ml) followed by a solution of chloride (1.1 equiv) obtained above in methylene chloride (30 ml) dropwise over a10-min period, and the solution was detected by TLC (AcOEt/DAB-6, 1:2 (V/V)). The mixture was condensed by rotary evaporation to remove the solvent. AcOEt (100 ml) was added to the product, and then it was washed followed by 1 N HCl, $NaHCO_3$ SS, brine to neutral, and dried by Na_2SO_4. It was filteered and condensed by rotary evaporation to obtain crude compound **3**, and then purified by column chromatography(AcOEt/DAB-6, 1:4 (V/V)) to obtain a colorless oil (3.1g), yield 86%.

The other N^6-[(benzyloxy)carbonyl]-N^2-L-lysine hexanoates were synthesized following the general procedure as described above.

Table 3. Main parameters of four CoMFA models

Model	Opt. Com.	q^2	R^2	F	SEE
A (all)	2	0.352	0.738	23.916	0.229
B (–**A7**)	2	0.316	0.753	24.346	0.229
C (–**B7**)	10	0.737	0.997	289.708	0.033
D (–**A7**, –**B7**)	9	0.728	0.995	189.744	0.042

N^6-[(Benzyloxy)carbonyl]- N^2 -(pyrazin-2-ylcarbonyl)-L-lysine hexanoate: (3.1 g, yield 86%).

N^6-[(Benzyloxy)carbonyl]-N^2-furoyl-L-lysine hexanoate: (2.9 g, yield 81%).

N^6-[(Benzyloxy)carbonyl]-N^2-(pyridin-3-ylcarbonyl)-L-lysine hexanoate: (3.0 g, yield 85%).

N^6-[(Benzyloxy)carbonyl]-N^2-(2-thienylcarbonyl)-L-lysine hexanoate: (3.2 g, yield 89%).

N^6-[(Benzyloxy)carbonyl]- N^2 -(2,4-dichlorobenzoyl)-L-lysine hexanoate: (3.3 g, yield 78%).

N^6-[(Benzyloxy)carbonyl]- N^2 -cinnamoyl-L-lysine hexanoate: (2.7 g, yield 68%).

N^6-[(Benzyloxy)carbonyl]- N^2-(3-nitrobenzoyl)-L-lysine hexanoate: (2.6 g, yield 65%).

N^6-[(Benzyloxy)carbonyl]- N^2-(4-nitrobenzoyl)-L-lysine hexanoate: (2.9 g, yield 79%).

N^6-[(Benzyloxy)carbonyl]-N^2-(4-bromobenzoyl)-L-lysine hexanoate: (3.0 g, yield 78%).

6.3.4. N^6-[(Benzyloxy)carbonyl]-N^2-isonicotinoyl-L-lysine (A1). Compound **3** 1.5 g was dissolved in methanol(20 ml), to the solution, 2 N NaOH (4 ml) was added. The solution was detected by TLC. The mixture was condensed by rotary evaporation to remove methanol, and then acidified to pH 4–6 by 1 N HCl, and then extracted by AcOEt (3× 150 ml). The mixture was dried by anhydrous Na_2SO_4, filtered and condensed by rotary evaporation to obtain the crude target compound. It was then recrystallized with AcOEt to give a white solid, yield 90.1%, mp 173–174 °C.ESI-MS 386.7 (M+H); ^{1}H NMR (DMSO-d_6, ppm): 12.699 (s, 1H, COOH), 8.904(d, J = 7.5 Hz, 1H, CONH), 8.736 (d, = 6.0 Hz, 2H, ArH), 7.788 (dd, = 1.50, 4.50 Hz, 2H, ArH), 7.293–7.379 (m, 5H, ArH), 7.250–7.269 (m, 1H, CONH), 4.988 (s, 2H, CH_2), 4.337 (q, = 13.80 Hz, 1H, CH), 2.992 (q, = 12.48 Hz, 2H, CH_2), 1.796–1.822 (m, 2H, CH_2), 1.296–1.411 (m, 4H, CH_2).

The other compounds of A series were synthesized following the general procedure as described above.

6.3.5. N^6-[(Benzyloxy)carbonyl]-N^2-(pyrazin-2- ylcarbonyl)-L-lysine (A2). White solid, yield 88.9%, mp 134–135 °C. ESI-MS 387.6 (M+H); ^{1}H NMR (DMSO-d_6, ppm): 12.852 (s, 1H, COOH), 9.188 (d, J = 1.5 Hz, 1H, ArH), 8.906 (s, 1H, ArH), 8.874 (d, J = 7.4 Hz, 1H, CONH); 8.761 (dd, = 1.50 Hz, 2.40Hz, 1H, ArH), 7.288–7.372 (m, 5H, ArH), 7.242–7.261 (m, 1H, CONH), 4.974 (s, 2H, CH_2), 4.434 (q, J = 13.60 Hz, 1H, CH), 2.967 (q, J = 12.37 Hz, 2H, CH_2), 1.848–1.873 (m, 1H, CH_2), 1.311–1.415 (m, 4H, CH_2).

6.3.6. N^6-[(Benzyloxy)carbonyl]-N^2-2-furoyl-L-lysine (A3). Yellow oil, yield 83.3%.ESI-MS 375.5 (M+H); ^{1}H NMR (DMSO-d_6, ppm): 12.637 (s, 1H, COOH), 8.421 (d, J = 7.8 Hz, 1H, CONH), 7.851 (d, = 0.3 Hz, 1H, ArH), 7.272–7.381 (m, 5H, ArH), 7.236–7.254 (m, 1H, CONH), 7.175 (d, = 3.60 Hz, 1H, ArH); 6.633 (dd, J = 1.80, 1.50 Hz, 1H, ArH); 4.990 (s, 2H, CH_2), 4.293 (q, J = 13.72 Hz, 1H, CH), 2.977 (q, J = 12.45 Hz, 2H, CH_2), 1.726–1.773 (m, 2H, CH_2), 1.236–1.392 (m, 4H, CH_2).

6.3.7. N^6-[(Benzyloxy)carbonyl]-N^2-(pyridin-3-ylcarbonyl)-L-lysine (A4). White solid, yield 93%, mp 175.5–176.5 °C. ESI-MS 386.7 (M+H); ^{1}H NMR (DMSO-d_6, ppm): 12.621 (s, 1H, COOH), 9.031 (d, J = 2.1 Hz, 1H, ArH), 8.809 (d, J = 7.80 Hz, 1H, CONH), 8.713–8.734 (m, 1H, ArH), 8.197–8.236 (m, 1H, ArH), 7.517 (dd, J = 4.80 Hz, 3.3 Hz, 1H, ArH), 7.291–7.379 (m, 5H, ArH), 7.250–7.269 (m, 1H, CONH), 4.985 (s, 2H, CH_2), 4.350 (q, J = 13.78 Hz, 1H, CH), 2.992 (q, J = 12.37 Hz, 2H, CH_2), 1.741–1.816 (m, 2H, CH_2), 1.356–1.467 (m, 4H, CH_2).

6.3.8. N^6-[(Benzyloxy)carbonyl]-N^2-(2-thienylcarbonyl)-L-lysine (A5). White solid, yield 81.5%, mp 58–60 °C. ESI-MS 391.5 (M+H); ^{1}H NMR (DMSO-d_6, ppm): 12.637 (s, 1H, COOH), 8.595 (d, J = 7.80 Hz, 1H, CONH), 7.892 (d, J = 3.0 Hz, 1H, ArH), 7.769 (d, J = 5.10 Hz, 1H, ArH), 7.293–7.381 (m, 5H, ArH), 7.250–7.269 (m, 1H, CONH), 7.158 (dd, J = 3.60, 1.20 Hz, 1H, ArH), 4.991 (s, 2H, CH_2), 4.296 (q, J = 13.56 Hz, 1H, CH), 2.987 (q, J = 12.39 Hz, 2H, CH_2), 1.716–1.821 (m, 2H, CH_2), 1.337–1.406 (m, 4H, CH_2).

6.3.9. N^6-[(Benzyloxy)carbonyl]-N^2-(2,4-dichlorobenzoyl)-L-lysine (A6). White solid, yield 86%, mp 130–131 °C. ESI-MS 453.4 (M+H); ^{1}H NMR (DMSO-d_6, ppm): 12.671 (s, 1H, COOH), 8.756 (d, J = 7.80 Hz, 1H, CONH), 7.681 (d, J = 1.80 Hz, 1H, ArH), 7.480–7.514 (m, 1H, ArH), 7.299–7.435 (m, 6H, ArH), 7.241–7.299 (m, 1H, CONH), 4.992 (s, 2H, CH_2), 4.304 (q, = 13.27 Hz, 1H, CH), 2.988 (q, J = 12.45 Hz, 2H, CH_2), 1.641–1.771 (m, 2H, CH_2), 1.211–1.286 (m, 4H, CH_2).

6.3.10. N^6-[(Benzyloxy)carbonyl]-N^2-cinnamoyl-L-lysine (A7). White solid, yield 82.7%, mp 56–57 °C. ESI-MS 411.6 (M+H); ^{1}H NMR (DMSO-d_6, ppm): 12.628 (s, 1H, COOH); 8.352 (d, = 7.8 Hz, 1H, CONH); 7.463–7.586 (m, 2H, Ar–H); 7.302–7.447 (m, 9H, ArH, =CH); 7.248–7.286 (m, 1H, NH); 6.748 (d, J = 15.9 Hz, 1H, =CH); 4.996 (s, 2H, CH_2); 4.290 (q, J = 13.58 Hz, 1H, CH); 2.977 (q, J = 12.29 Hz, 2H, CH_2); 1.618–1.765(m, 2H, CH_2); 1.329–1.420 (m, 4H, CH_2).

6.3.11. N^6-[(Benzyloxy)carbonyl]-N^2-(3-nitrobenzoyl)-L-lysine (A8). Yellow oil, yield 77.6%.ESI-MS 430.6 (M+H); ^{1}H NMR (DMSO-d_6, ppm): 12.596 (s, 1H, COOH), 9.020 (d, = 7.50 Hz, 1H, CONH), 8.742 (s, 1H, ArH); 8.413 (d, J = 8.10 Hz, 1H, ArH); 8.333 (d, = 7.80 Hz, 1H, ArH); 7.795 (t, J = 8.10 Hz, 1H, ArH); 7.324–7.374 (m, 5H, ArH); 7.265–7.288 (m, 1H, CONH), 4.982 (s, 2H, CH_2), 4.380 (q, J = 13.97 Hz, 1H, CH), 2.988 (q, J = 12.58 Hz, 2H, CH_2), 1.812–1.990 (m, 2H, CH_2), 1.234–1.420 (m, 4H, CH_2).

6.3.12. N^6-[(Benzyloxy)carbonyl]-N^2-(4-nitrobenzoyl)-L-lysine (A9). Yellow solid, yield 82.7%, mp 47–49 °C. ESI-MS 430.6 (M+H); ^{1}H NMR (DMSO-d_6, ppm): 12.687 (s, 1H, COOH), 8.950 (d, J = 7.50 Hz, 1H, CONH), 8.329 (d, J = 8.70 Hz, 2H, ArH); 8.116 (d, J = 8.70 Hz, 2H, ArH); 7.291–7.379 (m, 5H, ArH); 7.246–7.266 (m, 1H, CONH), 4.982 (s, 2H, CH_2), 4.365 (q, J = 13.85 Hz, 1H, CH), 3.001 (q, J = 12.47 Hz, 2H, CH_2), 1.809–1.991 (m, 2H, CH_2), 1.152–1.233 (m, 4H, CH_2).

6.3.13. N^6-[(Benzyloxy)carbonyl]-N^2-(4-bromobenzoyl)-L-lysine (A10). White solid, yield 83%, mp 140–141 °C. ESI-MS 465.4 (M+H); ^{1}H NMR (DMSO-d_6, ppm): 12.603 (s, 1H, COOH), 8.671 (d, J = 7.80 Hz, 1H, CONH), 7.832 (d, J = 8.10 Hz, 2H, ArH); 7.689 (d, J = 8.10 Hz, 2H, ArH); 7.292–7.377 (m, 5H, ArH); 7.238–7.276 (m, 1H, CONH), 4.983 (s, 2H, CH_2), 4.319 (q, J = 13.80 Hz, 1H, CH), 2.973 (q, J = 12.41 Hz, 2H, CH_2), 1.733–1.779 (m, 2H, CH_2), 1.352–1.427 (m, 4H, CH_2).

6.3.14. N^6-[(Benzyloxy)carbonyl]-N^2-isonicotinoyl-N^1-hydroxy-L-lysinamide (B1). This compound was prepared as described by Hwan[15] with compound **3**, the other compounds of A series were synthesized following the general procedure of **B1**.

White solid, yield 81%, mp 175–177 °C. ESI-MS 401.6 (M+H); ^{1}H NMR (DMSO-d_6, ppm): 10.743 (s, 1H, CONH), 8.873 (d, J = 1.50 Hz, OH); 8.792 (d, J = 8.10 Hz, 1H, CONH), 8.712 (dd, J = 1.50, 4.50 Hz, 2H, ArH), 7.786 (dd, J = 1.50 Hz, 4.50 Hz, 2H, ArH), 7.294–7.380 (m, 5H, ArH), 7.235–7.274 (m, 1H, CONH), 4.984 (s, 2H, CH_2), 4.312 (q, J = 13.64 Hz, 1H, CH), 2.973 (q, J = 12.35 Hz, 2H, CH_2), 1.673–1.744 (m, 2H, CH_2), 1.266–1.416 (m, 4H, CH_2).

6.3.15. N^6-[(Benzyloxy)carbonyl]-N^2-(pyrazin-2-ylcarbonyl)-N^1-hydroxy-L-lysinamide(B2). White solid, yield 73.3%, mp 55–57 °C. ESI-MS 402.6 (M+H); ^{1}H NMR (DMSO-d_6, ppm): 10.801 (s, 1H, CONH), 9.184 (d, J = 1.50 Hz, 1H, OH), 8.962 (s, 1H, ArH); 8.899 (d, J = 2.40 Hz, 1H, ArH), 8.755 (d, J = 1.50, 2.40 Hz, 1H, ArH); 8.576 (d, J = 8.40 Hz, 1H, CONH), 7.278–7.377 (m, 5H, ArH), 7.226–7.264 (m, 1H, CONH), 4.975 (s, 2H, CH_2), 4.395 (q, J = 13.72 Hz, 1H, CH), 2.959 (q, J = 12.49 Hz, 2H, CH_2), 1.689–1.762 (m, 1H, CH_2), 1.234–1.435 (m, 4H, CH_2).

6.3.16. N^6-[(Benzyloxy)carbonyl]-N^2-2-furoyl-N^1-hydroxy-L-lysinamide (B3). White solid, yield 80%, mp 55–57 °C. ESI-MS 390.6 (M+H); ^{1}H NMR (DMSO-d_6, ppm): 10.700 (s, 1H, CONH), 8.858 (s, 1H, OH); 8.206 (d, J = 8.40 Hz, 1H, CONH), 7.837 (d, J = 1.2 Hz, 1H, ArH), 7.282–7.384 (m, 5H, ArH), 7.233–7.269 (m, 1H, CONH), 7.201 (d, J = 3.30 Hz, 1H, ArH); 6.617(dd, J = 1.50, 3.30 Hz, 1H, ArH); 4.989 (s, 2H, CH_2), 4.270 (q, J = 13.63 Hz, 1H, CH), 2.963 (q, = 12.37 Hz, 2H, CH_2), 1.631–1.678 (m, 2H, CH_2), 1.151–1.423 (m, 4H, CH_2).

6.3.17. N^6-[(Benzyloxy)carbonyl]-N^2-(pyridin-3-ylcarbonyl)-N^1-hydroxy-L-lysinamide (B4). White solid, yield 82.4%, mp 142–143 °C. ESI-MS 401.6 (M+H); ^{1}H NMR (DMSO-d_6, ppm): 10.740 (s, 1H, CONH), 9.286 (s, 1H, OH); 9.033 (s, 1H, ArH), 8.706 (d, J = 7.20 Hz, 2H, ArH), 8.220 (d, J = 7.80 Hz, 1H, CONH); 7.496 (dd, J = 4.80, 5.10 Hz, 1H, ArH), 7.295–7.383 (m, 5H, ArH), 7.240–7.275 (m, 1H, CONH), 4.989 (s, 2H, CH_2), 4.334 (q, J = 13.56 Hz, 1H, CH), 2.973 (q, J = 12.24 Hz, 2H, CH_2), 1.703–1.751 (m, 2H, CH_2), 1.198–1.360 (m, 4H, CH_2).

6.3.18. N^6-[(Benzyloxy)carbonyl]-N^2-(2-thienylcarbonyl)-N^1-hydroxy-L-lysinamide (B5). White solid, yield 73%, mp 65–67 °C. ESI-MS 406.6 (M+H); ^{1}H NMR (DMSO-d_6, ppm): 10.714 (s, 1H, CONH), 8.852 (s, 1H, OH); 8.506 (d, J = 8.10 Hz, 1H, CONH), 7.921 (d, J = 2.70 Hz, 1H, ArH), 7.753 (dd, J = 0.9, 4.80 Hz, 1H, ArH), 7.274–7.383 (m, 5H, ArH), 7.236–7.254 (m, 1H, CONH), 7.139 (dd, J = 3.90, 4.80 Hz, 1H, ArH), 4.988 (s, 2H, CH_2), 4.268 (q, J = 13.72 Hz, 1H, CH), 2.960 (q, J = 12.78 Hz, 2H, CH_2), 1.643–1.730 (m, 2H, CH_2), 1.226–1.433 (m, 4H, CH_2).

6.3.19. N^6-[(Benzyloxy)carbonyl]-N^2-(2,4-dichlorobenzoyl)-N^1-hydroxy-L-lysinamide (B6). White solid, yield 77.8%, mp 172–173 °C. ESI-MS 468.5 (M+H); ^{1}H NMR (DMSO-d_6, ppm): 10.707 (s, 1H, CONH), 8.910 (s, 1H, OH); 8.760 (d, J = 8.10 Hz, 1H, CONH), 7.658 (d, J = 1.80 Hz, 1H, ArH), 7.445–7.493 (m, 2H, ArH), 7.301–7.367 (m, 5H, ArH), 7.237–7.273 (m, 1H, CONH), 4.992 (s, 2H, CH_2), 4.266 (q, J = 13.52 Hz, 1H, CH), 2.975 (q, J = 12.42 Hz, 2H, CH_2), 1.610–1.657 (m, 2H, CH_2), 1.288–1.398 (m, 4H, CH_2).

6.3.20. N^6-[(Benzyloxy)carbonyl]-N^2-cinnamoyl-N^1-hydroxy-L-lysinamide (B7). White solid, yield 74.8%, mp 168–169 °C. ESI-MS 426.5 (M+H); ^{1}H NMR (DMSO-d_6, ppm): 10.723 (s, 1H, CONH); 8.868 (d, J = 1.50 Hz, 1H, OH); 8.279 (d, J = 8.40 Hz, 1H, NH); 7.539–7.566 (m, 2H, Ar–H); 7.288–7.450 (m, 9H, Ar–H, =CH); 7.232–7.269 (m, 1H, NH); 6.768 (d, J = 15.9 Hz, 1H, =CH); 4.992 (s, 2H, CH_2); 4.260 (q, J = 13.63 Hz, 1H, CH); 2.967 (q, J = 12.46 Hz, 2H, CH_2); 1.537–1.607 (m, 2H, CH_2); 1.359–1.427 (m, 2H, CH_2); 1.240–1.315 (m, 2H, CH_2).

6.3.21. N^6-[(Benzyloxy)carbonyl]-N^2-(3-nitrobenzoyl)-N^1-hydroxy-L-lysinamide (B8). White solid, yield 60%, mp 177–179 °C. ESI-MS 445.7 (M+H); ^{1}H NMR (DMSO-d_6, ppm): 10.765 (s, 1H, CONH), 8.932 (d, J = 7.50 Hz, 1H, OH); 8.856 (d, J = 7.50 Hz, 1H, CONH), 8.752 (s, 1H, ArH); 8.392 (d, J = 8.10 Hz, 1H, ArH); 8.326 (d, J = 7.50 Hz, 1H, ArH); 7.771 (t, J = 8.10 Hz, 1H, ArH); 7.290–7.375 (m, 5H, ArH); 7.236–7.269 (m, 1H, CONH), 4.980 (s, 2H, CH_2), 4.346 (q, J = 13.67 Hz, 1H, CH), 2.975 (q, J = 12.49 Hz, 2H, CH_2), 1.693–1.765 (m, 2H, CH_2), 1.274–1.424 (m, 4H, CH_2).

6.3.22. N^6-[(Benzyloxy)carbonyl]-N^2-(4-nitrobenzoyl)-N^1-hydroxy-L-lysinamide (B9). White solid, yield 53.3%, mp 184–186 °C. ESI-MS 445.7 (M+H); ^{1}H NMR (DMSO-d_6, ppm): 10.081 (s, 1H, CONH), 9.083 (s, 1H, OH), 8.869 (d, J = 7.50 Hz, 1H, CONH), 8.325 (d, J = 8.70 Hz, 2H, ArH); 8.114 (d, J = 8.70 Hz, 2H, ArH); 7.263–7.371 (m, 5H, ArH); 7.227–7.236 (m, 1H, CONH), 4.988 (s, 2H, CH_2), 4.321 (q, J = 13.85 Hz, 1H, CH), 2.985 (q, J = 12.47 Hz, 2H, CH_2), 1.657–1.880 (m, 2H, CH_2), 1.079–1.381 (m, 4H, CH_2).

6.3.23. N^6-[(Benzyloxy)carbonyl]-N^2-(4-bromobenzoyl)-N^1-hydroxy-L-lysinamide (B10). White solid, yield 70%, mp 157–159 °C. ESI-MS 480.4 (M+H); ^{1}H NMR (DMSO-d_6, ppm): 10.701 (s, 1H, CONH), 8.840 (d, J = 1.20 Hz, 1H, OH); 8.553 (d, J = 8.10 Hz, 1H, CONH), 7.833 (d, J = 8.70 Hz, 2H, ArH); 7.667 (d, J = 8.40 Hz, 2H, ArH); 7.296–7.382 (m, 5H, ArH); 7.232–7.269 (m, 1H, CONH), 4.982 (s, 2H, CH_2), 4.291 (q, J = 13.72 Hz, 1H, CH), 2.969 (q, J = 12.34 Hz, 2H, CH_2), 1.678–1.707 (m, 2H, CH_2), 1.235–1.412 (m, 4H, CH_2).

Acknowledgments

This work was supported by the National Natural Foundation Research Grant (Grant Nos. 30772654 and 36072541) and the National High Technology Research and Development Program of China (863 project; Grant No. 2007AA02Z314) and Doctoral Foundation of Ministry of Education of the People's Republic of China (Grant No. 20060422029) and the Shandong Nature Science Foundation of China (Grant No. Y2004C02).

References and notes

1. Umezawa, H.; Aoyagi, T.; Suda, H.; Hamada, M. *Antibiotics* **1976**, *29*, 97–99.
2. Aoyagi, T.; Yoshida, S.; Nakamura, Y.; Shigihara, Y. *Antibiotics* **1990**, *43*, 143–148.
3. Rich, D. H.; Moon, B. J.; Harbeson, S. *J. Med. Chem.* **1984**, *27*, 417–422.
4. Umezawa, H.; Aoyagi, T.; Tanaka, T.; Suda, H. *Antibiotics* **1985**, *38*, 1629–1630.
5. Nagai, M.; Kojima, F.; Naganawa, H. *Antibiotics* **1997**, *50*, 82–84.
6. Lampret, B. R.; Kidric, J.; Kralj, B. *Arch. Microbiol.* **1999**, *171*, 397–404.
7. Chung, M. C.; Lee, H. J.; Chun, H. K. *Biosci. Biotechnol. Biochem.* **1996**, *60*, 898–900.
8. Aoyagi, T.; Yoshida, S.; Matsuda, N. *Antibiotics* **1991**, *44*, 573–578.
9. Egan, M. E.; Pearson, M.; Weiner, S. A. *Science* **2004**, *304*, 600–602.
10. Shim, J. S.; Lee, H.; Shin, J. *Cancer Lett.* **2004**, *203*, 163–169.
11. Qian, B. L.; Hao, F.; Wen, F. X. *Biol. Med. Chem. Lett.* **2007**, *17*, 2935–2938.
12. Cramer, R. D.; Patterson, D. E.; Bunce, J. D. *J. Am. Chem. Soc.* **1988**, *110*, 5959–5967.
13. Maciej, A.; Donald, D. J.; Rajarathnam, E. R. *Tetrahedron: Asymm.* **2000**, *11*, 2289–2298.
14. Jordis, U.; Sauter, F.; Siddiqi, S. M. *Ind. J. Chem. Sec. B* **1989**, 294–296.
15. Hwan, M. K.; Dong, K. R.; Yongseok, C. *J. Med. Chem.* **2007**, *50*, 2737–2741.